Mid-infrared Imaging of a Circumstellar Disk Around HR 4796: Mapping the Debris of Protoplanetary Accumulation

D.W. Koerner
183-501 Jet Propulsion Laboratory, 4800 Oak Grove Dr., Pasadena, CA 91109
University of Pennsylvania, Dept. of Physics & Astronomy,
4N14 DRL, 209 S. 33rd St., Philadelphia, PA 19104-6396
davidk@laplace.physics.upenn.edu

M.E. Ressler
169-327 Jet Propulsion Laboratory, 4800 Oak Grove Dr., Pasadena, CA 91109
ressler@cougar.jpl.nasa.gov

M.W. Werner
266-727 Jet Propulsion Laboratory, 4800 Oak Grove Dr., Pasadena, CA 91109
mww@ipac.caltech.edu

and D.E. Backman
Franklin & Marshall College, Dept. of Physics & Astronomy,
PO Box 3003, Lancaster, PA 17604-3003
Dana@astro.fandm.edu

Abstract

We report the discovery of a circumstellar disk around the young A0 star, HR 4796, in imaging carried out at thermal infrared wavelengths. By fitting a model of the emission from a flat dusty disk to the image at λ = 20.8 μm, we find the disk to be inclined $\imath = 72^{\circ}{}^{+6^{\circ}}_{-9^{\circ}}$ from face on with the long axis of emission oriented at PA $28^{\circ} \pm 6^{\circ}$. The intensity of emission does not decrease with radius as expected for circumstellar disks, but *increases* outward from the star, peaking near both ends of the elongated structure. We match this intensity pattern by varying the inner radius in our model and find the disk to have an inner hole with radius 55$\pm$15 AU. This radius is similar to that of the region enclosed by the inner edge of our own Kuiper belt and may suggest a source of the dust in the collision of cometesimals. By contrast with the emission at 20.8 μm, the morphology at λ = 12.5 μm is far more concentrated. A residual image from the model subtraction at 20.8 μm shows similar excess emission close to the star. The intensity and ratio of flux densities at the two wavelengths indicates that a very tenuous component of dust with mean temperature of a few hundred degrees K is confined within a few AU of the star. This location corresponds to that of zodiacal dust in our own solar system and may indicate a similar source for the emission. The morphology of dust emission from HR 4796 suggests that its disk (age 10 Myr) is in a transitional planet-forming stage, between that of massive gaseous proto-stellar disks like that around the Herbig Ae star MWC 480, and more tenuous debris disks such as the one detected around the much older (400 Myr) A0 star, Vega. The HR 4796 disk was discovered independently and contemporaneously by Jayawardhara et al. (1998).

1 Introduction

It is now well over a decade since coronagraphic imaging of stellar light scattered by a disk around β Pictoris provided circumstantial evidence for the recent birth of an extra-solar planetary system (Smith & Terrile 1984). Since then, coronagraphic and adaptive-optics (AO) searches have continued the quest for additional examples (Smith, Fountain, & Terrile 1992; Kalas & Jewitt 1995; Mouillet, et al. 1997), but none have been successful at imaging light scattered by dust around similar IRAS-selected candidates (see Table VII from Backman & Paresce 1993, for example). This failure was originally interpreted to suggest that the disk around β Pic is highly unusual (Smith & Terrile 1992), but subsequent identification of a few other main sequence A stars with fractional infrared excesses of the same magnitude has been used to argue that ∼20% of all A-type stars pass through an early phase like that of β Pic (Jura et al. 1998). If true, the failure to image other candidates is likely due to their greater distance; limitations in current coronagraphic techniques would prevent detection of even β Pic's disk if it were several times farther away (cf. Kalas & Jewitt 1996). An alternative approach is suggested by successful imaging of the thermal dust emission from the disk around β Pic at mid-infrared wavelengths (Lagage & Pantin 1994; Pantin, Lagage, & Artymowicz 1997). As part of an effort to take full advantage of this relatively new technique, we present thermal infrared imaging of the circumstellar environment of HR 4796, a more distant A0 star (Houk 1982) suggested to have a disk similar to that of β Pic on the basis of its IRAS excess (Jura 1991; Jura et al. 1993; 1995; 1998).

At a distance of 67±3 pc (π = 14.91±0.75 mas; Hipparcos Catalog), HR 4796 is three and a half times farther away than β Pic (D = 19.3±0.2 pc; π = 51.87±0.51 mas), but exhibits a strong IRAS excess with optical depth estimated to be twice as large (Jura 1991). No circumstellar disk is immediately apparent in recent images at optical wavelengths obtained with HST/WFPC2 (Krist et al. 1997), ground-based AO-coronagraphy (Mouillet, et al. 1997), or HST/NICMOS coronagraphy (B.A. Smith, private communication). An M dwarf companion is detected 7.7″ (∼ 500 AU) from the star, however, and is believed to be physically bound on the basis of common proper motion (Jura et al. 1993). The age of the system is estimated to be t = 10 Myr on the basis of isochrone fitting (Jura et al. 1998), in keeping with its identification as an outlying member of the Centaurus-Lupus association (Jura et al. 1993) with average age t = 12-15 Myr (de Geus, De Zeeuw, & Lub 1989). This age is younger than other well-known members of the Vega class ($t \sim$ 100 Myr) and suggests that HR 4796 may be somewhat transitional between young Herbig Ae stars ($t \sim$ 1Myr) with optically thick disks (Mannings & Sargent 1997; Mannings, Koerner, & Sargent 1997) and "Vega-type" stars (cf. Backman & Paresce 1993).

2 Observations and Results

We observed HR 4796 with JPL's mid-infrared camera MIRLIN at the F/40 bent-Cassegrain focus of the Keck II telescope on UT 16 March 1998. MIRLIN employs a Boeing 128×128 pixel, high-flux Si:As BIB detector with a plate scale at Keck II of 0.137″ per pixel. The latter was determined by scanning a star across both MIRLIN's field-of-view and that of the Keck II guide camera for which the plate scale has been accurately measured. The associated field of view was 17.5″. Background subtraction was carried out by chopping the secondary mirror at a ∼4 Hz rate with 8″ throw in the north-south direction and by nodding the telescope a similar distance in the

east-west direction after coadding a few hundred chop pairs. With this setup, an image of the source was always on the array; double-differenced frames were imprinted with four images of the source, two positive and two negative. These were shifted and added with the appropriate sign to make the final 64 × 64 (8.3″ × 8.3″) images. Observations were carried out in filters centered at λ = 12.5, 20.8, and 24.5 μm with widths 1.2, 1.7, and 0.8 μm respectively. At 12.5 μm, 5 integrations of duration 18 ms were coadded at each of the chop positions and summed over 200 chop cycles before nodding. At 20.8 and 24.5 μm, respectively, 5 and 3 integrations with duration 15 and 25 ms were coadded in 300 chop cycles before nodding. Small dither steps were taken between chop-nod cycles. Observations of infrared standards α Sco, σ Sco, and α Lyr were observed in the same way at similar airmasses. An additional sequence of images was obtained by alternating rapidly between the 12.5 and 20.8 μm filters with no telescope offsets in order to accurately determine the registration between the two wavelengths.

The resulting images of HR 4796 are displayed in Figure 1 together with corresponding images of a standard star for comparison. At λ = 12.5 μm, peak flux density of 184±18 mJy is located at the position of the star and comprises nearly all of the point-like emission rising above a low-level plateau. The fainter emission accounts for an additional 40 mJy and is slightly extended to the NE and SW. We estimate the stellar photospheric emission to be 122 mJy at this wavelength, implying both that the total excess is nearly equal to that of the photospheric emission and that an excess that is 50% of photospheric levels arises from very near the star. In the corresponding image at 20.8 μm, emission is elongated $\sim$3″ in diameter at PA 30° with total flux density 1.88±0.2 Jy, consistent with the 20μm bolometer measurement of Jura et al. (1993) (1.86 Jy). Our 24.5 μm measurements are not of sufficient signal to noise to merit display, but show a size and orientation consistent with that in Fig. 1. Total flux density is 2.27±0.7 Jy.

Surprisingly, the center of the 20.8 μm structure is not coincident with the peak emission, but is at the locus of a very weak emission peak centered between two larger ones located at either end. It is evident in Figure 2, a two-color rendition of the combined images, that the peak 12.5 μm emission is centered on the 20.8 μm source as well. Below, we interpret this morphology as arising from a nearly edge-on circumstellar disk with an inner hole and investigate its properties with the aid of a simple model.

3 Modeling and Interpretation

Our measured flux densities are listed in Table I and plotted in Figure 3 together with color-corrected IRAS measurements and an upper limit obtained with the JCMT at λ = 800 μm by Jura et al. (1993). The spectral distribution of the flux densities exhibits a nearly black-body shape which peaks at $\lambda \approx 60\mu$m, well away from the maximum stellar photosphere emission. It can be reproduced by emission from a model disk with mass approximately 1.0 $M_\oplus$, if the disk is largely devoid of radiating particles inside a radius of a few times 10 AU (Jura et al. 1995; 1998). In order to uniquely constrain the spatial distribution of dust, however, it is desirable to gain the maximum amount of information from images which resolve the circumstellar material.

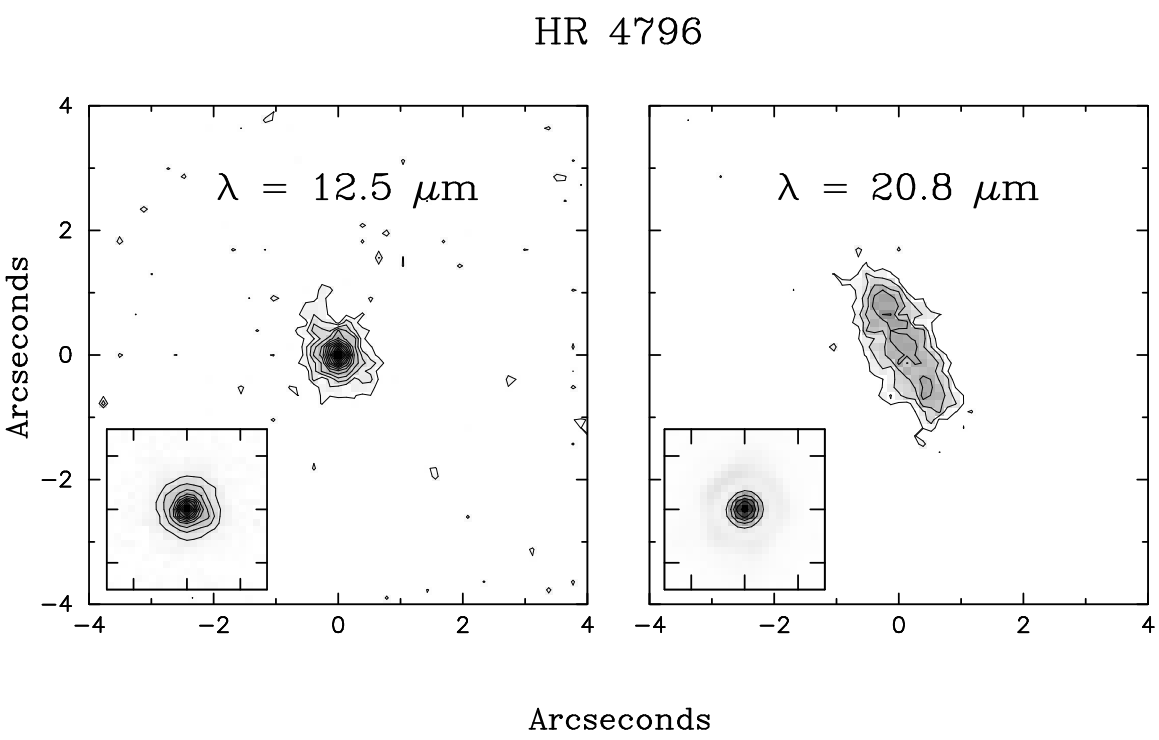

Figure 1: Contour plots of the intensity of emission from HR 4796 at λ = 12.5 and 20.8 μm. Contours are at 2 σ intervals, starting at 3 σ. Images of standard stars taken in the same filters and at the same approximate time and airmass are shown in the lower left corner of each frame for comparison.

Table 1: Flux Densities for HR 4796

λ_{eff} (μm)	$\delta\lambda$ (μm)	Flux Density (Jy)	Uncertainty (Jy)	Photosphere (Jy)	Excess (Jy)
12.5	1.2	0.223	0.018	0.122	0.101±0.018
20.8	1.7	1.880	0.170	0.047	1.813±0.170
24.5	0.8	2.270	0.700	0.033	1.994±0.700
12.0	6.5	0.309	0.028	0.136	0.173±0.028
25.0	11.0	3.280	0.13	0.032	3.250±0.130
60.0	40.0	8.640	0.43	0.006	8.630±0.430
100.0	37.0	4.300	0.34	0.002	4.300± 0.340
800.0[1]	100.0	< 0.028	–	–	–

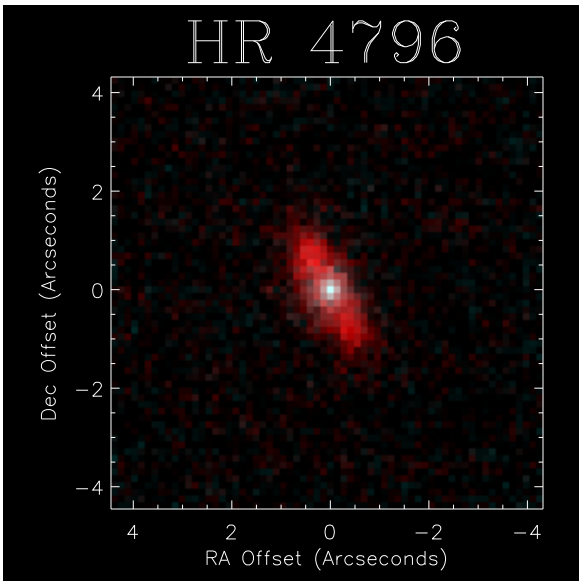

Figure 2: Composite 2-color image of the emission from HR 4796 at λ = 12.5 (cyan) and 20.8 μm (red). Registration was accomplished by taking images at the same telescope position and rapidly cycling between both filters.

The optically thin radiation from an annulus of width dr and radius r in a flat dusty circumstellar disk is estimated by Backman, Gillett, & Witteborn (1992) to be

$$f(r) = \tau_{r_0}\left(\frac{r}{r_0}\right)^{\gamma}\varepsilon_\lambda\, B[T_p(r),\lambda]\left(\frac{2\pi r dr}{D^2}sr\right)Jy,$$

where τ_{r_0} is the geometrical optical depth perpendicular to the disk plane at a fiducial radius r_0, T_p is the particle temperature, ε_λ is the particle radiative efficiency relative to a black body, and D the 67 pc distance to HR 4796. For a distribution of grains with effective size, λ_0, we assume $\varepsilon_\lambda = 1$ for $\lambda < \lambda_0$ and $\varepsilon_\lambda = (\lambda/\lambda_0)^{-1}$ for $\lambda > \lambda_0$ (see Appendix D of Backman et al. (1992) for the relation between λ_0 and a particle size distribution). The grain temperature is then $T_p(r) = 468(L_*/\lambda_0)^{0.2}(r/1\mathrm{AU})^{-0.4}$ where L_* is the stellar luminosity in solar units. Based on IRAS color temperatures, λ_0 lies in the range 40–80μm; we assume λ_0 = 60 μm. For M_V = 5.80, D = 67 pc, and assuming 54 $L_\odot$ for a star with the same temperature as α Lyr, L_* = 18.1 $L_\odot$. Parameters which remain to be determined include the power-law index of the optical depth, γ, inner and outer radii, r_{in} and r_{out}, τ_{r_0}, inclination angle ι (from face on), and position angle θ.

The morphology of the 20.8 μm emission in Fig. 1 provides a useful constraint on r_{in}, ι, θ, and τ_{r_0} under the assumption of a single power-law structure to the radial optical depth. However, it does little to constrain r_{out}, γ, and λ_0. The latter can be better determined from fits to the flux density distribution, especially if values of the former can be derived from a fit to the image. In both cases, we choose to evaluate the uncertainties in the range of acceptable parameter values by calculating the probability of the models given the data. We use the above formulation to simulate both the image and the flux density distribution and calculate the reduced χ^2 over the range of parameter values. The associated probability of the data given the model is taken to be $P = e^{-\chi^2}$.

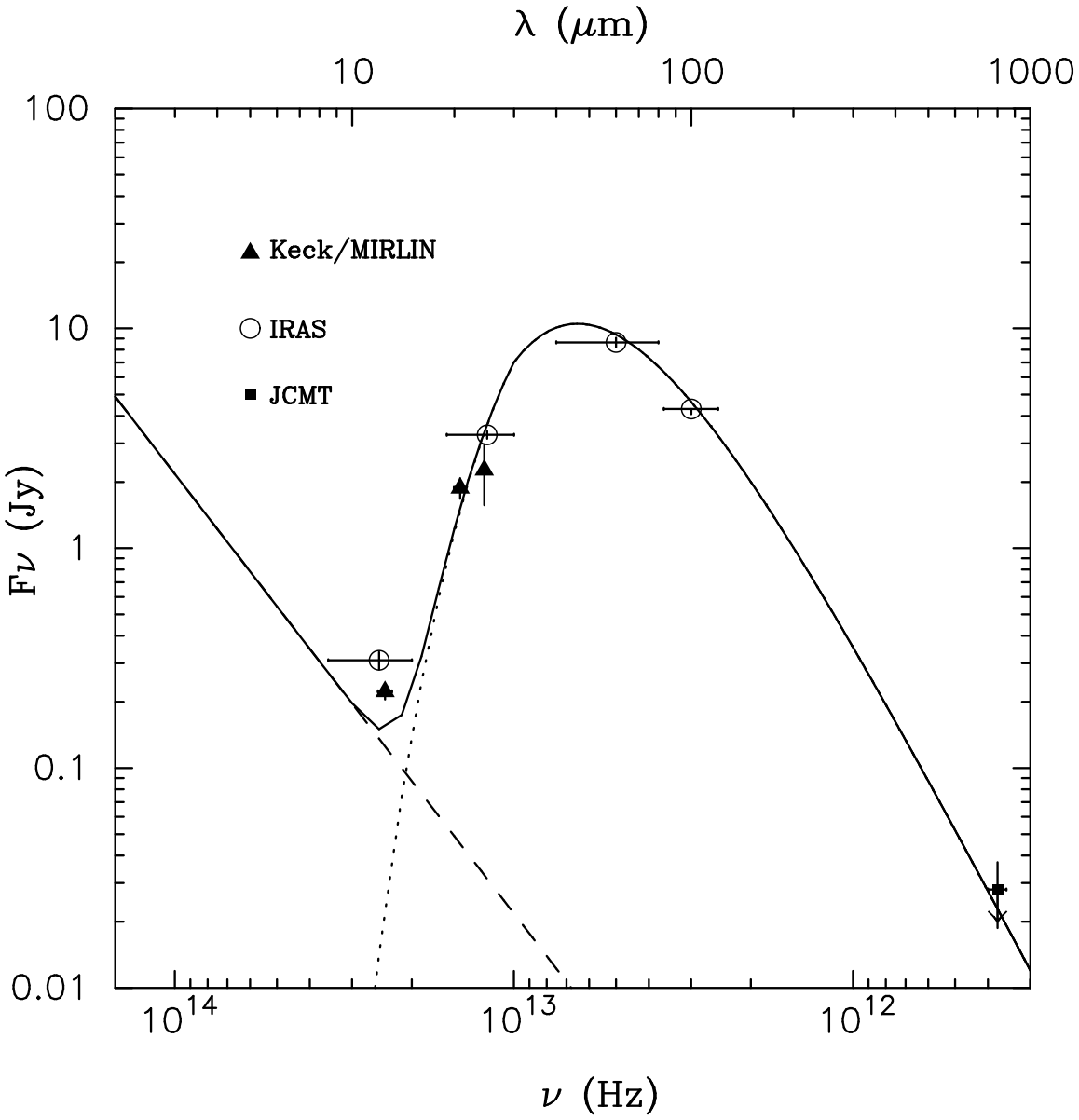

Figure 3: Plot of the flux densities for HR 4796 listed in Table I. The solid curve marks the total emission from the stellar photosphere (dashed line) and a model of the emission from a disk with 55 AU inner hole (dotted line).

The probability of the model given the data is then estimated by summing and normalizing the probabilities over the whole range of parameter space considered. For the estimate of ι, individual probabilities are scaled by $\cos(\iota)$ to account for the *a priori* expectation that the system is oriented edge on (see Lay et al. 1997 for a more detailed description of this Bayesian approach).

3.1 Image Simulations at $\lambda = 20.8\mu$m

To simulate the image of HR 4796 at 20.8μm, we assumed a thin disk with emission as prescribed above, calculated the contribution at each point of an evenly-spaced 9×9 grid per pixel (Δs = 1/8th of a pixel), and summed the result in each of 64×64 pixels corresponding to the image. A flux density corresponding to that of the stellar photosphere was added to the central pixel, and the model image was convolved with that of a standard star which was obtained at similar air mass and within a short time of the HR 4796 observations. The resulting image was then subtracted from the data and the squared difference weighted by the noise to derive reduced χ^2 and P in the usual way. Initial disk parameter values were estimated from the distribution of flux densities in order to determine orientation parameters ι and θ. The most likely values of these were then taken in a second model fit while varying r_{in}, τ_{r_0}, and γ. Assuming the best values from the latter, a repeat fit to ι and θ was completed as a check.

The final results for ι and θ agreed with the initial ones and are displayed in plots of the probability distribution for each parameter displayed in Fig. 4. We find $\iota = 72^\circ{}^{+6^\circ}_{-9^\circ}$ and $\theta = 28^\circ \pm 6^\circ$. The reliability of these estimates is contingent on the suitability of the 2-dimensional model; if the disk is particularly thick, estimates of the inclination with a thinner model would lead to an overestimate of its departure from an edge-on orientation. Strictly speaking, the estimate of ι is thus an upper limit to the deviation from a purely edge-on orientation.

Our primary aim in modeling the morphology of the 20.8 μm emission is to test for the presence of an inner hole in the disk and refine an estimate of its dimensions. For this purpose, we deemed it necessary to also consider a range of values for γ and τ_{r_0}, since these affect the radial distribution and intensity of emission from the disk. The value of γ was varied between 0 and -2.5 and τ_{r_0} was considered over the range $10^{-5} < \tau_{50AU} < 10$. The appearance of the 20.8 μm emission is not sensitive to increases in the choice of outer radii larger than the boundary of emission in the image, since the temperature rapidly decreases to levels at which emission is negligible at that wavelength; we adopted r_{out} = 125 AU. The resulting estimate of r_{in} is evident in the plot in Fig. 5. It is clear from this figure that the source of emission in Fig. 1 cannot extend inward to within 20 AU of the star as an extrapolation of a single power-law profile to the radial optical depth. In fact, the inner radius of the disk is estimated to be a good deal larger, $r_{in} = 55\pm15$AU. The reliability of this result is bolstered by the fact that the 30 AU total uncertainty in the value of r_{in} corresponds to the angular resolution of the observations, 0.45″, and by the result that the choice of power-law index for the geometrical optical depth has little effect on the final estimate.

The most probable model is displayed together with the data and residuals in the color plate in Fig. 6. It is apparent that, although the presence of a hole leads to a good match with the outer disk, some emission close to the star remains in the residual image. This emission looks similar to the 12.5 μm image in appearance and may have a common origin in a warmer population of dust grains near the star with greatly decreased geometrical optical depth relative to that of the outer disk. The unresolved flux density in excess of the stellar photosphere is 62 mJy at λ = 12.5 μm;

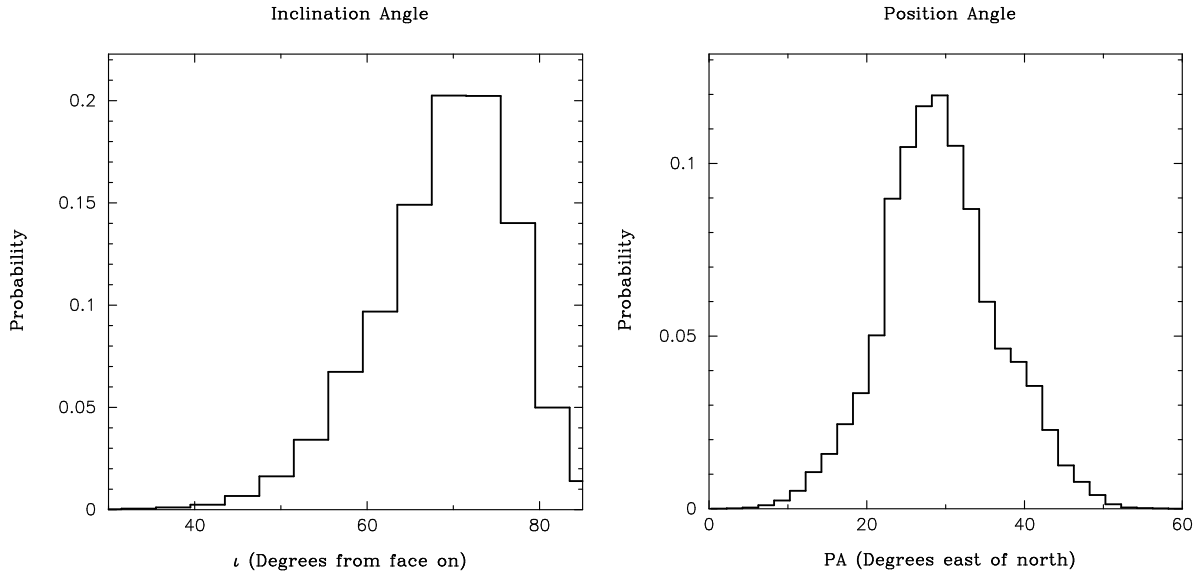

Figure 4: Plots of the probability distributions for values of ι, the angle of disk inclination with respect to a face-on orientation (left), and the Position Angle of the long axis of emission in degrees east of north (right).

excess residual flux density at λ = 20.8 μm is 96 mJy. These values suggest a mean temperature of 250 K and associated distance from the star of 3.1 AU if the grains have the same size as in the outer disk, 5.7 AU if they have sizes commensurate with the ability to radiate as black body grains. It holds in either case that the majority of grains giving rise to the emission lie well interior to the 55-AU radius of the hole and in a radial zone which corresponds to that of the zodiacal dust in our own solar system.

3.2 Modeling the Flux Densities with Imaging Constraints

The properties of the outer regions of dusty circumstellar disks are best estimated with measurements of their emission at far infrared and millimeter wavelengths which probe cold dust (cf. Beckwith et al. 1990). Assuming an inner radius derived from our fit to the high-resolution 20.8 μm image, we try to estimate these properties with a model of the spectral distribution of flux densities. In addition to IRAS fluxes and an upper limit at λ = 800 μm, our measurements in narrow bands at λ = 12.5, 20.8, and 24.5 μm provide new constraints on the distribution of material. Our image at 12.5 μm demonstrates further that much of the infrared excess at that wavelength does *not* arise from the "disk" outside r_{in} = 55 AU. Consequently, we do not attempt to fit either that measurement or the IRAS 12 μm flux density with our disk model.

We varied four parameters, τ_{50AU}, γ, r_{out}, and λ_0, over the ranges, $10^{-5} < \tau_{50AU} < 10$, -4.5$< \gamma, 0$, 56AU$< r_{out} <$200AU, and 10$\mu$m$< \lambda_0 <$ 80μm in a fit to all flux densities at wavelengths longer than 20 μm plotted in Fig. 3. Flux from the inner region was derived from a fit to the "point-source" flux densities at 12.5 and 20.8 μm and subtracted (89, 88, 23, and 6 mJy at 24.5, 25, 60, and 100 μm). The scatter in the data about the model curve exceeds the formal uncertainties quoted for the

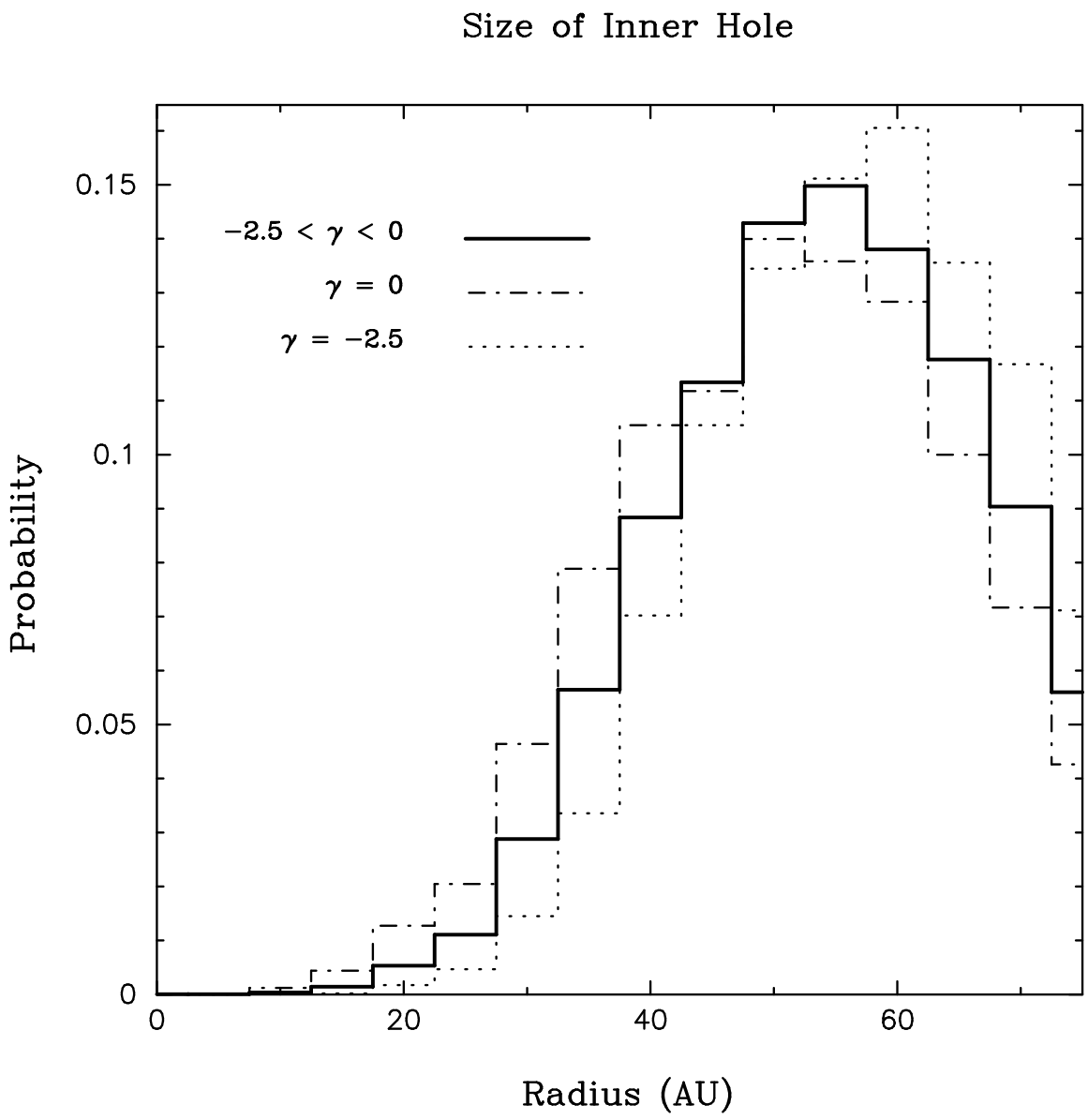

Figure 5: Plot of the probability distribution for values of the radius of an inner hole in the disk. As described in the text, the radial power-law index of the geometric optical depth was also varied from γ = -2.5 to 0.0. The distribution over all values of γ is shown as a solid line. That for γ = 0.0 is plotted as a dashed and dotted line, and for γ = -2.5 as a dotted line.

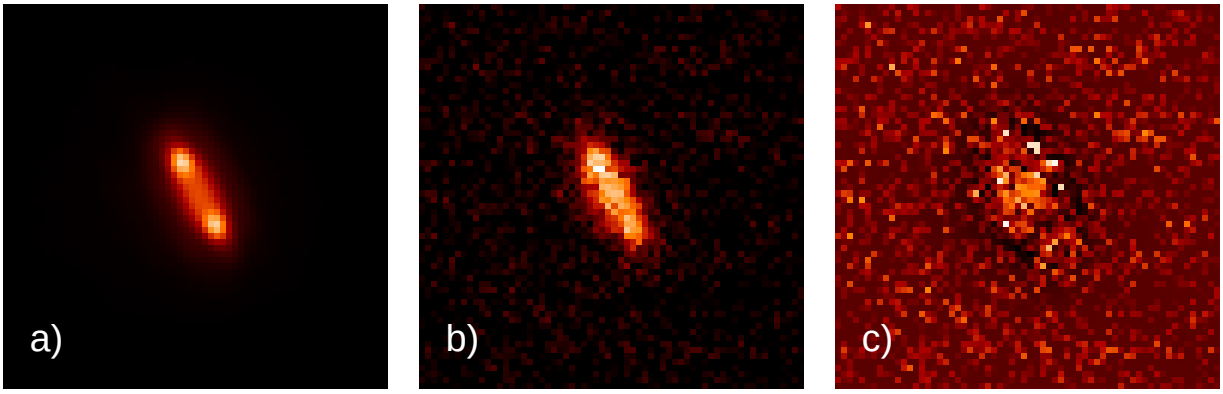

Figure 6: a) Model of the 20.8 μm emission from a flat dusty disk with a 55 AU inner hole and a central star with flux density matched to that of HR 4796. The model was generated as described in the test and convolved with a PSF derived from a standard star. b) Image of 20.8 μm emission from HR 4796. c) Residuals from the subtraction of the model from the image. Excess 20.8 μm emission near the star has a flux density of 96 mJy.

measurements by factors of several. Consequently, it is difficult to attach a meaning to the width of the probability distributions for each of the parameter values; we do not plot those here. If the scatter in the data about the best-fit model is taken as a measure of the true uncertainty, the most narrowly preferred values over the entire distribution are r_{out} = 57 AU and $\lambda_0 \approx 10-40\mu$m. Broad distributions leave τ_{50AU} and γ almost completely undetermined. A ring this concentrated and narrow is likely to be too short-lived to be likely, however, and the non-uniqueness of this choice of parameter values can be illustrated by the fact that associated parameters can be found for an outer radius of 80 AU that give nearly as close a fit as a model with the most probable parameter values. An example is plotted in Fig. 3 and is calculated assuming r_{in} = 55 AU, r_{out} = 80 AU, λ_0 = 30 μm, τ_{50AU} = 0.065 and γ = -2.0.

4 Discussion

Our observations provide direct evidence for the existence of a disk around the young A0 star, HR 4796, with size and orientation that agree with the results of an independent simultaneous discovery (Jayawardhana et al. 1998). The morphology of emission in our images at λ = 20.8 μm also reveals an inner hole in the disk with radius 55$\pm$15 AU. Emission in excess above the photosphere at 12.5 μm, however, predominantly arises from a region interior to this radius. When compared to the residual 20.8 μm emission at this location, the 12.5 μm radiation yields an estimate of the source temperature of a few hundred K, corresponding to a radial distance of a few AU from the central star. Taken together, the properties of the disk around HR 4796 are startlingly like those believed to have existed in the late bombardment stage of the early solar system, when collisions between cometesimals in the outer solar system and between planetesimals or asteroids in a terrestrial planet-forming zone were likely to have generated a large population of smaller dust grains distributed in much the same way as those imaged around HR 4796.

Given the properties we derive for the disk around HR 4796, its null detection in scattered light by coronagraphic means is not surprising (Krist et al. 1997; Mouillet, et al. 1997). A prediction of the detectability of the disk with this technique is obtained with the aid of estimates of the bolometric luminosity ratio, L_{dust}/L_*, estimated characteristic grain size, and a range of disk radii from the distribution of flux densities. Subject to an error dictated largely by the uncertainty in the grain albedo, this calculation verifies the detectability of β Pic due to its proximity and density. Using optical coronagraph data and modeling the corresponding detection limits, however, Kalas & Jewitt (1996) concluded that even an edge-on disk around HR 4796 with twice the scattering optical depth of β Pic (estimated from L_{dust}/L_*) would go undetected due to its distance 3.5 times farther away.

The existence of planetary systems around stars such as HR 4796 which are slightly more massive than the sun is supported by recent molecular line surveys of Herbig Ae stars with mm-wave interferometry (Mannings & Sargent 1997; Mannings et al. 1997). These confirm the presence of disks with properties very like those around the less-massive T Tauri stars (Koerner & Sargent 1996) with ages of 10^5 to a few times 10^6 yr. The mass of gas and dust in such disks often exceeds that of the "minimum mass solar nebula" capable of giving rise to a solar system like our own. In contrast, no molecular gas was detected recently in measurements of HR 4796 (Zuckerman, Forveille, & Kastener 1995), and the total mass of emitting particles is many times less. This could be explained if the material around HR 4796 has accumulated into large bodies which contribute little to the disk emission, though comprising most of the circumstellar mass. As outlined here, the radial distribution of dust in the HR 4796 disk supports such a notion by analogy with our solar system. Its 10 Myr age is intermediate between that of the Herbig Ae stars and Vega-type stars with far more tenuous debris disks. These facts are well explained by a simple picture in which HR 4796 is surround by a disk in transition from a gaseous protoplanetary stage to that in which young planets are fully formed.

Acknowledgments

We wish to thank Robert Goodrich and the WMKO summit staff for their many hours of assistance in helping to adapt MIRLIN to the Keck II visitor instrument port. Operator assistants Ron Quick and Joel Aycock were especially helpful in developing work-arounds for the operational vagaries introduced by the Keck/MIRLIN pairing. We especially thank Keck Observatory Director F.Chaffee for supporting the use of MIRLIN at Keck.

We are very grateful to M. Jura for many helpful discussions and to the team from the Center for Astrophysics and the University of Florida (R.Jayawardhana, C.Telesco, G.Fazio, L.Hartmann, R.Pena, and S.Fisher) for sharing their results prior to publication. Development of MIRLIN was supported by the JPL Director's Discretionary Fund and by an SR+T award from NASA's Office of Space Science. The use of MIRLIN at the Keck Observatory was supported by an award from NASA's Origins program. We thank J.Bock, G.Reyes, and J. Van Cleve (Cornell University) for assisting in the development of MIRLIN.

References

Backman, D.E., & Paresce, F., 1993, in Protostars and Planets III, (ed. E.H. Levy and J.I. Lunine), Tucson: University of Arizona Press, p. 1253

de Geus, E.J., de Zeeuw, P.T., & Lub, J., 1989, A&A, 216, 44

Houk, N., 1982, in Michigan Spectral Catalog (Ann Arbor: Univ. of Michigan Press), p. 3

Jayawardhana, R., Telesco, C., Faxio, G., Hartmann, L., Pena, R., Fisher, S., 1998, ApJsubmitted.

Jura, M., 1991, ApJ, 383, L79

Jura, M., Zuckerman, B., Becklin, E.E., & Smith, R.C. 1993, ApJ, 418, L37

Jura, M., Ghez, A.M., White, R. J., McCarthy, D.W., Smith, R.C., & Martin, P.G., 1995, ApJ, 445, 451

Jura, M., Malkan, M., White, R., Telesco, C., Pena, & Fisher, R.W. 1998, ApJ, in press.

Kalas, P., & Jewitt, D., 1995, Ap&SS, 223, 167

Kalas, P., & Jewitt, D., 1996,AJ, 111, 1347

Krist, J.E., Burrows, C.J., Stapelfeldt, K.R., et al., 1997, BAAS, 191, 05.14

Lagage, P.O., & Pantin, E., 1994, Nature, 369, 628

Mannings, V., & Sargent, A.I., 1997, ApJ, 490, 792

Mannings, V., Koerner, D.W., & Sargent, A.I., 1997, Nature, 388, 555

Mouillet, A., Lagrange, A.-M., Beuzit, J.-L., & Renaud, N., 1997, A&A, 324, 1083

Pantin, E., Lagage, P.O., & Artymowicz, P., 1997, A&A, 327, 1123

Smith, B.A., Fountain, J.W., & Terrile R.J., 1992, A&A, 261, 499

Smith, B.A., & Terrile R.J., 1984, Science, 226, 4681

Stauffer, J.R., Hartmann, L.W., & Barrado y Navascues, D., 1995, ApJ, 454, 910

Zuckerman, B., Forveille, T., & Kastner, J.H., 1995, Nature, 373, 6514